

# DESIGN SUSTAINABLE ADAPTIVE SLIDING MODE CONTROLLER ON THE FUZZY NEURONS BASIS FOR ELECTROLYTIC COPPER GANTRY CRANE

Van Trung Nguyen<sup>1</sup>, Van Vang Do<sup>1</sup>, Quyet Thang Le<sup>1</sup>,  
Thi Thanh Huyen Phi<sup>1</sup>, Van Cuong Pham<sup>2,\*</sup>

DOI: <https://doi.org/10.57001/huih5804.2026.003>

## ABSTRACT

Gantry cranes used in copper electrolysis function as robotic systems in factories, transporting and assembling cathode and anode plates. Due to the thick arrangement of electrolyte panels, crane movements often result in significant fluctuations, leading to positional inaccuracies and potential safety issues. This paper presents a sustainable adaptive sliding mode controller based on fuzzy neurons to minimize vibration and improve the positioning accuracy of the electrolytic copper gantry crane system (ECGCS). Sliding Mode Control (SMC) is a nonlinear directional control method known for its stability and robustness, even under system disturbances or changing crane parameters. However, large control amplitudes can lead to chattering near the sliding surface. To address this issue, the proposed control strategy incorporates three types of Radial Basis Function Neural Networks (RBFNNs) for online estimation of nonlinear control functions, combined with fuzzy logic to determine the appropriate control law magnitude. The system adapts its parameters using Lyapunov stability theory to ensure both accuracy and long-term durability. Simulation results in MATLAB Simulink demonstrate that the proposed controller provides high precision, reduced vibration and strong durability.

**Keywords:** Gantry crane; Sliding mode control; Fuzzy control; Neural networks; Robust adaptive control; Genetic Algorithm.

<sup>1</sup>Faculty of Electricity, Quang Ninh University of Industry, Vietnam

<sup>2</sup>Hanoi University of Industry, Vietnam

\*Email: [cuongpv0610@hauai.edu.vn](mailto:cuongpv0610@hauai.edu.vn)

Received: 18/10/2025

Revised: 14/12/2025

Accepted: 28/01/2026

## 1. INTRODUCTION

In the era of industrialization, the demand for iron, nonferrous metals, and other basic materials has

increased significantly. To transport these materials efficiently, gantry cranes have become indispensable. The electrolytic copper gantry crane, as illustrated in Figure 1, is not only used for transporting electrolytic plates but also plays a crucial role in assembling them into slots inside electric tank stools or other robotic systems. Ensuring that the electrolytic plates are transported and assembled safely, efficiently, and on time is essential. As a result, numerous studies have been conducted to improve the performance of gantry cranes.

Structurally, overhead gantry cranes were moved by a forklift, with the load suspended from the forklift via a cable [1-6]. These cranes performed the functions of lifting, lowering, and horizontal movement. However, the natural swinging of the load-resembling a pendulum motion-significantly reduced their operational efficiency [7]. The swaying of the load is primarily caused by the movement of the forklift, frequent changes in cable length, variations in load mass, and external disturbances such as wind or collisions. To address these issues, numerous studies have focused on developing control strategies for automated crane operation, aiming to minimize swing angles, reduce transport time, and improve positioning accuracy. Among these, adaptive control methods have shown promising results [8-11]. PID controllers are widely used in industrial control systems due to their simple structure, ease of tuning, and good stability. To optimize the PID controller parameters for crane systems, various algorithms such as Particle Swarm Optimization (PSO), Differential Evolution (DE), and Genetic Algorithm (GA) have been proposed [12-15]. In [16, 17], a Fuzzy-PID control approach was introduced, combining the advantages of both PID and fuzzy controllers. This hybrid method performs particularly well

when the system approaches the setpoint, especially under conditions of large deviation, where its nonlinear characteristics enable a very fast response.

Additionally, fuzzy control techniques have demonstrated successful results in real-world applications, including gantry crane systems [18-20]. For example, the Dual PD dimming controller [21] uses the first fuzzy controller to regulate the position of the cart, while the second controller manages the payload's sway angle. This approach achieves fast positioning and effectively minimizes load sway. In [22], a double fuzzy control method was shown to reduce sway angles significantly; however, it required a longer time to reach the desired positions. Sliding mode controllers, as reported in [23, 24], provide stable and robust performance even under system disturbances or time-varying parameter changes. Nevertheless, a major drawback of sliding mode control is the chattering phenomenon caused by large control amplitudes around the sliding surface. To address this issue, many researchers have proposed fuzzy sliding mode controllers [25-34], which combine the benefits of both control strategies to reduce chattering and improve system performance. The results show that the crane can quickly move to the desired position while effectively controlling the oscillation of small loads and eliminating the chattering phenomenon around the sliding surface. However, the fuzzy controller's rules are typically based on the designer's experience, which can lead to instability and difficulty in achieving optimal control performance. Moreover, these rules cannot be precisely described using mathematical models. Relying solely on expert knowledge is often insufficient, making it challenging to develop an optimal control law. To address this issue, several studies have proposed a robust adaptive sliding mode controller based on neural networks for gantry crane systems [35, 36]. This controller inherits the advantages of the neural controller, particularly its ability to learn rules online during operation. In this paper, to improve control efficiency and accelerate convergence speed, we propose a fuzzy sliding mode controller combined with adaptive control based on Radial Basis Function Neural Networks (RBFNNs) to control the Electrolytic Copper Gantry Crane System (ECGCS). In the proposed controller, RBFNNs and fuzzy logic are utilized to estimate the nonlinear functions and the control law amplitude, respectively. The adaptive update law for the network parameters is derived using Lyapunov stability theory. Furthermore, simulation results demonstrate that

the proposed controller achieves high accuracy, reduced vibrations, and enhanced robustness.

This paper is organized as follows. Section 2 presents the dynamic modeling of the gantry crane system for copper electrolysis. Section 3 develops a robust adaptive sliding mode controller based on fuzzy neural networks. Section 4 provides the simulation results. Finally, Section 5 concludes the paper.



Figure 1. Picture of the ECGCS

## 2. MODEL THE DYNAMICS OF THE CRANE GANTRY SYSTEM FOR COPPER ELECTROLYSIS

A gantry crane electrolytic copper system is shown in Figure 2, the parameters and values are taken in proportion to the actual value as shown in Table 1. This system can be modeled as a trolley with mass  $M$ . A hook attached to it has a mass  $m_1$ ,  $l_1$  is hook cable length. The electrolytic plate attached to the hook has a mass  $m_2$ ,  $l_2$  is 1/2 electrolytic plate length,  $\theta_1$  is the hook swing angle versus the vertical line,  $\dot{\theta}_1$  is the angular velocity of the hook,  $\theta_2$  is the swing angle of the electrolytic plate compared to the vertical line,  $\dot{\theta}_2$  is the angular velocity of the electrolytic plate. The crane moves with a thrust  $F$ (N). Assumption of massless and rigid cables, mass-point hooks and mass-point electrolytic plates.

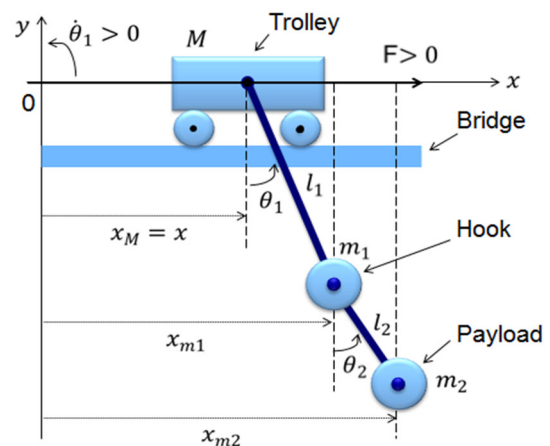


Figure 2. Diagram of the ECGCS

According to the Lagrangian equation:

$$\frac{d}{dt} \left( \frac{\partial L}{\partial \dot{q}_i} \right) - \frac{\partial L}{\partial q_i} = Q_i \tag{1}$$

Where:  $L = T - P$ ,  $T$  is the kinetic energy of the system,  $P$  is the potential of the system,  $q_i$  is the generalized system of coordinates,  $i$  is the number of degrees of freedom of the system,  $Q_i$  is the external force.

As shown in Figure 2, the kinetic energy of the system is given by:

$$\begin{aligned} T = T_M + T_{m1} + T_{m2} = & \frac{1}{2} M \dot{x}^2 \\ & + \frac{1}{2} m_1 (\dot{x}^2 + l_1^2 \dot{\theta}_1^2 + 2\dot{x}l_1\dot{\theta}_1 \cos\theta_1) \\ & + \frac{1}{2} m_2 (\dot{x}^2 + l_1^2 \dot{\theta}_1^2 + l_2^2 \dot{\theta}_2^2 + 2\dot{x}l_1\dot{\theta}_1 \cos\theta_1 \\ & + 2\dot{x}l_2\dot{\theta}_2 \cos\theta_2 + 2l_1l_2\dot{\theta}_1\dot{\theta}_2 \cos(\theta_1 - \theta_2)) \end{aligned} \tag{2}$$

The potential energy of the system are:

$$\begin{aligned} P = (m_1 + m_2)gl_1(1 - \cos\theta_1) \\ + m_2gl_2(1 - \cos\theta_2) \end{aligned} \tag{3}$$

Replace (2), (3) into (1), the nonlinear equation of the copper electrolytic gantry system can be described as follows [11, 24]:

$$(M + m_1 + m_2)\ddot{x} + (m_1 + m_2)l_1(\ddot{\theta}_1 \cos\theta_1 - \dot{\theta}_1^2 \sin\theta_1) + m_2l_2(\ddot{\theta}_2 \cos\theta_2 - \dot{\theta}_2^2 \sin\theta_2) = F + \sigma_d - \mu\dot{x} \tag{4}$$

$$\begin{aligned} (m_1 + m_2)l_1 \cos\theta_1 \ddot{x} + (m_1 + m_2)l_1^2 \ddot{\theta}_1 \\ + m_2l_1l_2 \ddot{\theta}_2 \cos(\theta_1 - \theta_2) + m_2l_1l_2 \dot{\theta}_2^2 \sin(\theta_1 - \theta_2) \\ + (m_1 + m_2)gl_1 \sin\theta_1 = 0 \end{aligned} \tag{5}$$

$$\begin{aligned} m_2l_2 \cos\theta_2 \ddot{x} + m_2l_1l_2 \ddot{\theta}_1 \cos(\theta_1 - \theta_2) + m_2l_2^2 \ddot{\theta}_2 \\ - m_2l_1l_2 \dot{\theta}_1^2 \sin(\theta_1 - \theta_2) + m_2gl_2 \sin\theta_2 = 0 \end{aligned} \tag{6}$$

Where:  $F$  is the external force acting on the crane system,  $\sigma_d$  expresses the bounded disturbance.

The dynamic Eqs. (4-6) can be rewritten as follows [11, 24]:

$$M(X)\ddot{X} + C(X, \dot{X})\dot{X} + G(X) = \tau + \sigma_d \tag{7}$$

Here  $X = [x \ \theta_1 \ \theta_2]^T = [x_1 \ x_3 \ x_5]^T$  is a vector of the generalized coordinate variables,  $(x_1, \dot{x}_1, \ddot{x}_1) \in R^{3 \times 1}$ ,  $(x_3, \dot{x}_3, \ddot{x}_3) \in R^{3 \times 1}$ ,  $(x_5, \dot{x}_5, \ddot{x}_5) \in R^{3 \times 1}$  respectively the position, velocity and acceleration of the trolley, angle, angular velocity, angular acceleration of the hook and electrolytic plate,  $\tau = [F \ 0 \ 0]^T$  is a vector of the generalized force,  $\sigma_d \in R^{3 \times 1}$  expresses the bounded disturbance vector,  $M(X) \in R^{3 \times 3}$  is a inertia matrix,  $C(X, \dot{X}) \in R^{3 \times 3}$  is a vector of Coriolis and centripetal torques, and  $G(X) \in R^{3 \times 1}$  is a vector of the gravitational term.  $M(X)$ ,  $C(X, \dot{X})$  and  $G(X)$  are determined by:

$$M(X) = \begin{bmatrix} M + m_{12} & m_{12}l_1C\theta_1 & m_2l_2C\theta_2 \\ m_{12}l_1C\theta_1 & m_{12}l_1^2 & m_2l_1l_2C\theta_{12} \\ m_2l_2C\theta_2 & m_2l_1l_2C\theta_{12} & m_2l_2^2 \end{bmatrix}$$

$$C(X, \dot{X}) = \begin{bmatrix} \mu & -m_{12}l_1\dot{\theta}_1S\theta_1 & -m_2l_2\dot{\theta}_2S\theta_2 \\ 0 & 0 & -m_2l_1l_2\dot{\theta}_2S\theta_{12} \\ 0 & -m_2l_1l_2\dot{\theta}_1S\theta_{12} & 0 \end{bmatrix}$$

$$G(X) = [0 \ m_{12}gl_1S\theta_1 \ m_2gl_2S\theta_2]^T$$

Where:  $m_1 + m_2 = m_{12}$ ;  $\cos\theta_1 = C\theta_1$ ;  $\sin\theta_1 = S\theta_1$ ;  $\cos\theta_2 = C\theta_2$ ;  $\sin\theta_2 = S\theta_2$ ;  $\cos(\theta_1 - \theta_2) = C\theta_{12}$ ;  $\sin(\theta_1 - \theta_2) = S\theta_{12}$

To design the controller, we offer properties for (7) as follows [11]:

**Property 1.** The inertial matrix  $M(X)$  is a positive symmetric matrix and bounded:

$$M(X) \leq m_0 I \tag{8}$$

Here  $m_0 > 0$  and  $m_0 \in R$

**Property 2.**  $\dot{M}(X) - 2C(X, \dot{X})$  is skew symmetric matrix, for any vector  $x$ :

$$x^T [\dot{M}(X) - 2C(X, \dot{X})] x = 0 \tag{9}$$

**Property 3.** The double-pendulum overhead crane system has one control input (trolley force  $F$ ), whereas the variables to be controlled are three (trolley position  $x$ , hook swing angle  $\theta_1$ , payload swing angle  $\theta_2$ ). Therefore, the double-pendulum overhead crane system is an under actuated nonlinear system.

**Property 4.** The double-pendulum overhead crane system is a passive system.

### 3. RBFNNs CONTROLLER DESIGN

Radial Basis Function (RBF) neural networks have attracted significant attention due to their strong generalization ability and simple network structure, which helps avoid unnecessary and lengthy computations. The structure of the RBFNNs, consisting of three layers, is illustrated in Figure 3.

Layer 1. The input layer. In this layer, input signals  $X = [x_1, x_2 \dots x_6]$  are moved directly to the next layer.

Layer 2. The hidden layer. Each neuron of the hidden layer is activated by a radial basis function. The output of hidden layer is calculated as follows:

$$h_{M(x_j)} = \exp\left(\frac{-\|x_j - c_i\|^2}{2\delta_i^2}\right) \tag{10}$$

$$h_{C(x_j, \dot{x}_j)} = \exp\left(\frac{-\|x_j - c_i\|^2}{2\delta_i^2}\right) \tag{11}$$

$$h_{G(x_j)} = \exp\left(\frac{-\|x_j - c_i\|^2}{2\delta_i^2}\right) \tag{12}$$

Where:  $x_j$  is an input vector,  $c_i$  is the center vector with the same dimension as  $x_j$ ,  $\delta_i$  is the variance of the basic function,  $i = 1, 2, 3; j = 1, 3, 5$  and if  $i = 1$  then  $j = 1$ , if  $i = 2$  then  $j = 3$ , if  $i = 3$  then  $j = 5$ .

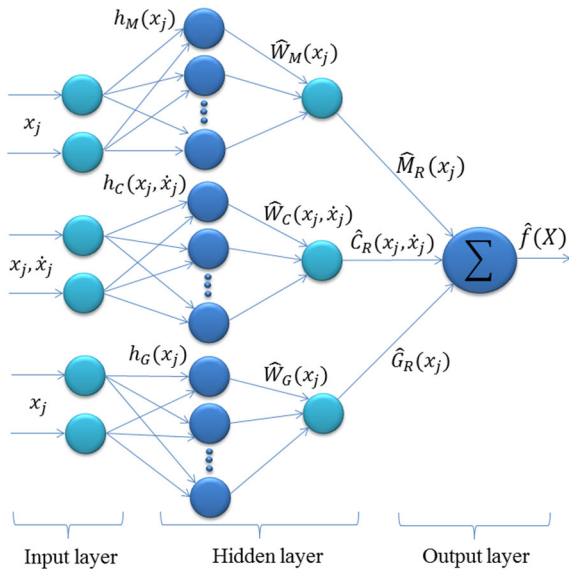


Figure 3. Controller structure RBFNNs

Layer 3. The output layer. We assume that the ideal output value of the RBFNNs controller is  $M_R(x_j)$ ,  $C_R(x_j, \dot{x}_j)$ ,  $G_R(x_j)$  and is calculated as:

$$\begin{aligned} M(x_j) &= M_R(x_j) + E_M(x_j) \\ &= W_{M(x_j)}^T * h_{M(x_j)} + E_M(x_j) \end{aligned} \quad (13)$$

$$\begin{aligned} C(x_j, \dot{x}_j) &= C_R(x_j, \dot{x}_j) + E_C(x_j, \dot{x}_j) \\ &= W_{C(x_j, \dot{x}_j)}^T * h_{C(x_j, \dot{x}_j)} + E_C(x_j, \dot{x}_j) \end{aligned} \quad (14)$$

$$\begin{aligned} G(x_j) &= G_R(x_j) + E_G(x_j) \\ &= W_{G(x_j)}^T * h_{G(x_j)} + E_G(x_j) \end{aligned} \quad (15)$$

Where:  $j = 1, 3, 5$ .  $W_{M(x_j)}$ ,  $W_{C(x_j, \dot{x}_j)}$ ,  $W_{G(x_j)}$  are the optimal weight value of the controller.  $h_{M(x_j)}$ ,  $h_{C(x_j, \dot{x}_j)}$ ,  $h_{G(x_j)}$  are the outputs of the hidden class.  $E_M(x_j)$ ,  $E_C(x_j, \dot{x}_j)$ ,  $E_G(x_j)$  are the errors of  $W_{M(x_j)}$ ,  $W_{C(x_j, \dot{x}_j)}$ ,  $W_{G(x_j)}$  respectively, and is limited.

Values of  $M_R(x_j)$ ,  $C_R(x_j, \dot{x}_j)$ ,  $G_R(x_j)$  are determined by the following formula:

$$\hat{M}_R(x_j) = \hat{W}_{M(x_j)}^T * h_{M(x_j)} \quad (16)$$

$$\hat{C}_R(x_j, \dot{x}_j) = \hat{W}_{C(x_j, \dot{x}_j)}^T * h_{C(x_j, \dot{x}_j)} \quad (17)$$

$$\hat{G}_R(x_j) = \hat{W}_{G(x_j)}^T * h_{G(x_j)} \quad (18)$$

Where:  $\hat{W}_{M(x_j)}$ ,  $\hat{W}_{C(x_j, \dot{x}_j)}$ ,  $\hat{W}_{G(x_j)}$  are the evaluation values of  $W_{M(x_j)}$ ,  $W_{C(x_j, \dot{x}_j)}$ ,  $W_{G(x_j)}$  respectively.

The output of the RBFNNs can be given by:

$$\begin{aligned} \hat{f}(X) &= \sum_{i=1}^3 \left[ W_{M(x_j)}^T * h_{M(x_j)} + E_M(x_j) \right] \\ &+ \sum_{i=1}^3 \left[ W_{C(x_j, \dot{x}_j)}^T * h_{C(x_j, \dot{x}_j)} + E_C(x_j, \dot{x}_j) \right] \\ &+ \sum_{i=1}^3 \left[ W_{G(x_j)}^T * h_{G(x_j)} + E_G(x_j) \right] \end{aligned} \quad (19)$$

The controller RBFNNs is designed for the ECGCS under the impact of force  $\tau$  the difference between the vector of the actual value  $x_1, x_3, x_5$  with the desired value  $x_{r1}, x_{r3}, x_{r5}$  have can be converged to 0 when  $t \rightarrow \infty$ . The structure of the control system for electrolytic copper gantry crane was designed as Figure 4:

Let  $x_{r1}, x_{r3}, x_{r5}$  correspond to the position, rotation angle of the hook, rotation angle of the desired electrolytic plate of the crane system,  $x_1, x_3, x_5$  are, respectively, actual output of gantry crane position, swing angle of the hook, swing angle of the electrolytic plate. The control objective is to take  $x_1, x_3, x_5$  to  $x_{r1}, x_{r3}, x_{r5}$  with the smallest error and the minimum load oscillation. Definition of control error as follows:

$$e_i = x_j - x_{rj} \quad (20)$$

Where:  $i = 1, 2, 3; j = 1, 3, 5$  and if  $i = 1$  then  $j = 1$ , if  $i = 2$  then  $j = 3$ , if  $i = 3$  then  $j = 5$ .

The sliding mode functions for the three subsystems are defined as follows:

$$s_i = \dot{e}_i + \lambda_i e_i = \dot{x}_{2i} + \lambda_i (x_j - x_{rj}) \quad (21)$$

Where:  $\lambda_i$  are positive real numbers.

The second slip surface is constructed as follows:

$$s = \sum_{i=1}^3 \alpha_i s_i = \sum_{i=1}^3 (\alpha_i \dot{x}_{2i} + \alpha_i \lambda_i (x_j - x_{rj})) \quad (22)$$

Where:  $\alpha_i$  are positive real numbers.

Substitution (18) into (7) we have:

$$\begin{aligned} M(x_j) \alpha_i \dot{s}_i + C(x_j, \dot{x}_j) \alpha_i s_i &= -M(x_j) \alpha_i \ddot{x}_{rj} \\ &- M(x_j) \alpha_i \lambda_i \dot{x}_{rj} - C(x_j, \dot{x}_j) \alpha_i \dot{x}_{rj} - C(x_j, \dot{x}_j) \alpha_i \lambda_i x_{rj} \\ &+ M(x_j) \alpha_i \lambda_i \dot{x}_j + C(x_j, \dot{x}_j) \alpha_i \lambda_i x_j - \alpha_i G(x_j) \\ &+ \alpha_i \tau_j + \alpha_i \sigma_{dj} \end{aligned} \quad (23)$$

Where:  $i = 1, 2, 3; j = 1, 3, 5$  and if  $i = 1$  then  $j = 1$ , if  $i = 2$  then  $j = 3$ , if  $i = 3$  then  $j = 5$ .

From (13-15) and (23) we have:

$$\begin{aligned} M(x_j) \alpha_i \dot{s}_i + C(x_j, \dot{x}_j) \alpha_i s_i &= f_i(X) + \tau_i \\ &+ E_i(X) + \sigma_{di} \end{aligned} \quad (24)$$

$$\begin{aligned} f_i(X) &= -M_R(x_j) \alpha_i \ddot{x}_{rj} - M_R(x_i) \alpha_i \lambda_i \dot{x}_{rj} \\ &- C_R(x_j, \dot{x}_j) \alpha_i \dot{x}_{rj} - C_R(x_j, \dot{x}_j) \alpha_i \lambda_i x_{rj} + M_R(x_j) \alpha_i \lambda_i \dot{x}_j \\ &+ C_R(x_j, \dot{x}_j) \alpha_i \lambda_i x_i - \alpha_i G(x_j) \end{aligned}$$

$$E_i(X) = -E_M(x_j)\alpha_i\ddot{x}_{rj} - E_M(x_j)\alpha_i\lambda_i\dot{x}_{rj} - E_C(x_j, \dot{x}_j)\alpha_i\dot{x}_{rj} - E_C(x_j, \dot{x}_j)\alpha_i\lambda_i x_{rj} + E_M(x_j)\alpha_i\lambda_i\dot{x}_i + E_C(x_j, \dot{x}_j)\alpha_i\lambda_i x_j - \alpha_i E_G(x_j)$$

$$\tau_i = \alpha_i \tau_j \text{ and } \sigma_{di} = \alpha_i \sigma_{dj}$$

From the diagram of the structure of the control system for electrolytic copper gantry crane Figure 4 we have:

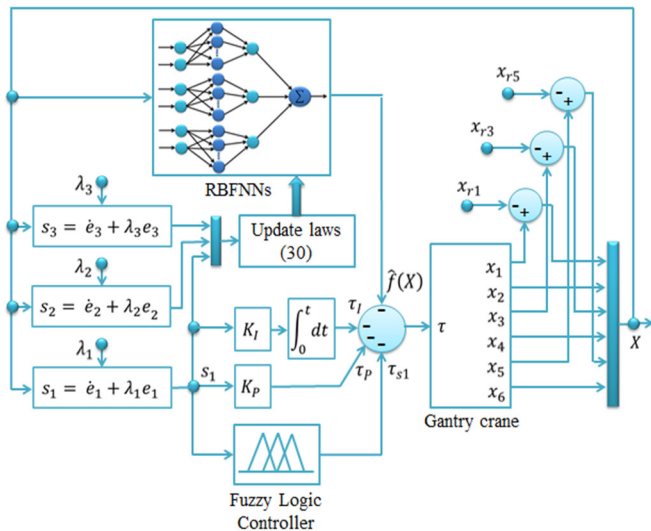


Figure 4. The structure of the control system

$$\tau = \sum_{i=1}^3 \tau_i = -\hat{f}(X) - \tau_{s1} - \tau_I - \tau_P \tag{25}$$

Where:  $\tau_i = \alpha_i K_i \int_0^t s_1 dt$ ,  $\tau_P = \alpha_i K_P s_1$ ,  $\hat{f}(X) = \sum_{i=1}^3 \hat{f}_i(X)$  is the output signal of the RBFNNs controller

$$\hat{f}_i(X) = -\hat{M}_R(x_j)\alpha_i\ddot{x}_{rj} - \hat{M}_R(x_j)\alpha_i\lambda_i\dot{x}_{rj} - \hat{C}_R(x_j, \dot{x}_j)\alpha_i\dot{x}_{rj} - \hat{C}_R(x_j, \dot{x}_j)\alpha_i\lambda_i x_{rj} + \hat{M}_R(x_j)\alpha_i\lambda_i\dot{x}_i + \hat{C}_R(x_j, \dot{x}_j)\alpha_i\lambda_i x_j - \hat{G}_R(x_j)\alpha_i$$

$\tau_{s1}$  the sliding mode controller (SMC) and selected as follows:

$$\tau_{s1} = \alpha_1 K_{s1} \text{sign}(s_1) \tag{26}$$

Where:

$$K_{s1} \geq \frac{1}{\alpha_1} [E_1(X) + E_2(X) + E_3(X) + \sigma_{d1} + \sigma_{d2} + \sigma_{d3}]$$

$$\text{sign}(s_1) = \begin{cases} 1 & \text{if } s_1 > 0 \\ -1 & \text{if } s_1 < 0 \\ 0 & \text{if } s_1 = 0 \end{cases} \tag{27}$$

In order to increase the cling efficiency and increase the convergence speed, we have designed the fuzzy sliding mode controller to combine with the RBFNNs controller as follows:

Based on equation (26), we choose  $\tau_{s1} = \alpha_1 K_1$  (28)

Where:

$$K_1 \geq \frac{1}{\alpha_1} [E_1(X) + E_2(X) + E_3(X) + \sigma_{d1} + \sigma_{d2} + \sigma_{d3}]$$

is the amplitude of the control law estimated online by the fuzzy inference system with the following fuzzy rules:

IF  $s_1$  is  $A^m$  THEN  $K_1$  is  $B^m$

Where:  $A^m$  and  $B^m$  is the fuzzy set (Figure 5).

The member functions used are the Gaussian function:

$$\mu_A(x) = \exp\left(-\left(\frac{x-\alpha}{\sigma}\right)^2\right) \tag{29}$$

Where:  $A$  is one of the fuzzy sets,  $\alpha, \sigma$  in turn is the center and width of the Gaussian function,  $x$  is  $s$  or  $K_1$ .  $K_1$  can be written as:

$$K_1 = \frac{\sum_{j=1}^l \theta_{K_1}^j \mu_{A^j}(s)}{\sum_{j=1}^l \mu_{A^j}(s)} = \theta_{K_1}^T \psi_{K_1}(s) \tag{30}$$

Where:  $\psi_{K_1}(s) = [\psi_{K_1}^1(s), \dots, \psi_{K_1}^l(s)]^T$  is the vector of the height of the membership functions of  $K_1$  in which  $\psi_{K_1}^l(s) = \mu_{A^l}(s) / \sum_{j=1}^l \mu_{A^j}(s)$ ,  $\theta_{K_1} = [\theta_{K_1}^1, \dots, \theta_{K_1}^l]^T$  is the vector of the center of the membership functions of  $K_1$ .

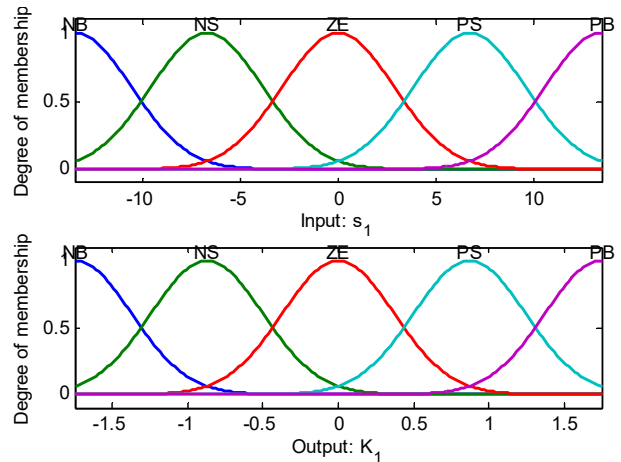


Figure 5. The membership functions of the input and output variables fuzzy controller

The range of input language variables is  $s_{1min} = -13.5, s_{1max} = 13.5$  and the range of the output language variable is  $K_{1min} = -1.75, K_{1max} = 1.75$ .

Both input and output variables are used in five fuzzy sets to describe is Negative Big (NB), Negative Small (NS), Zero (ZE), Positive Small (PS), and Positive Big (PB).

The fuzzy rules are defined as follows:

IF  $s_1$  is NB THEN  $K_1$  is NB

IF  $s_1$  is NS THEN  $K_1$  is NS

IF  $s_1$  is ZE THEN  $K_1$  is ZE

IF<sub>S1</sub> is PS THEN  $K_1$  is PS

IF<sub>S1</sub> is PB THEN  $K_1$  is PB

Substituting equation (23) to (22) we have:

$$M(x_j)\alpha_i\dot{s}_i + C(x_j, \dot{x}_j)\alpha_i s_i = \tilde{f}_i(X) - \tau_{s1} - \tau_l - \tau_p + E_i(X) + \sigma_{di} \quad (31)$$

$$\begin{aligned} \tilde{f}_i(X) &= f_i(X) - \hat{f}_i(X) = -\tilde{M}_R(x_j)\alpha_i\ddot{x}_{rj} \\ &- \tilde{M}_R(x_j)\alpha_i\lambda_i\dot{x}_{rj} - \tilde{C}_R(x_j, \dot{x}_j)\alpha_i\dot{x}_{rj} - \tilde{C}_R(x_j, \dot{x}_j)\alpha_i\lambda_i x_{rj} \\ &+ \tilde{M}_R(x_j)\alpha_i\lambda_i + \tilde{C}_R(x_j, \dot{x}_j)\alpha_i\lambda_i x_j - \tilde{G}_R(x_j)\alpha_i \end{aligned}$$

In order to stabilize the system in this article, the adaptive law of the RBFNNs controller is chosen as follows:

$$\begin{cases} \dot{\hat{W}}_{M(x_j)} = \beta_{M(x_j)} h_{M(x_j)} Z_1(X) \alpha_i s_i \\ \dot{\hat{W}}_{C(x_j, \dot{x}_j)} = \beta_{C(x_j, \dot{x}_j)} h_{C(x_j, \dot{x}_j)} Z_2(X) \alpha_i s_i \\ \dot{\hat{W}}_{G(x_j)} = -\beta_{G(x_j)} h_{G(x_j)} \alpha_i s_i \end{cases} \quad (32)$$

Where:  $-\ddot{x}_{rj} - \lambda_i\dot{x}_{rj} + \lambda_i\dot{x}_j = Z_1(X)$ ;

$-\dot{x}_{rj} - \lambda_i x_{rj} + \lambda_i x_j = Z_2(X)$

Consider the Lyapunov function has the equation as follows:

$$\begin{aligned} V(t) &= \frac{1}{2} \sum_{i=1}^3 s_i M(x_j) \alpha_i s_i + \frac{1}{2} \alpha_1 \left( \int_0^t s_1 dt \right) K_I \left( \int_0^t s_1 dt \right) \\ &+ \frac{1}{2} \sum_{i=1}^3 \beta_{M(x_j)}^{-1} \tilde{W}_{M(x_j)}^T \tilde{W}_{M(x_j)} \\ &+ \frac{1}{2} \sum_{i=1}^3 \beta_{C(x_j, \dot{x}_j)}^{-1} \tilde{W}_{C(x_j, \dot{x}_j)}^T \tilde{W}_{C(x_j, \dot{x}_j)} \\ &+ \frac{1}{2} \sum_{i=1}^3 \beta_{G(x_j)}^{-1} \tilde{W}_{G(x_j)}^T \tilde{W}_{G(x_j)} \end{aligned} \quad (33)$$

Where:  $\tilde{W}_{M(x_j)} = W_{M(x_j)} - \hat{W}_{M(x_j)}$ ;

$\tilde{W}_{C(x_j, \dot{x}_j)} = W_{C(x_j, \dot{x}_j)} - \hat{W}_{C(x_j, \dot{x}_j)}$ ;

$\tilde{W}_{G(x_j)} = W_{G(x_j)} - \hat{W}_{G(x_j)}$ .

First derivative V (t) over time we obtain the equation as follows:

$$\begin{aligned} \dot{V}(t) &= \frac{1}{2} \sum_{i=1}^3 s_i \dot{M}(x_j) \alpha_i s_i + \sum_{i=1}^3 s_i M(x_j) \alpha_i \dot{s}_i \\ &+ s_1 \alpha_1 K_I \int_0^t s_1 dt + \sum_{i=1}^3 \beta_{M(x_j)}^{-1} \tilde{W}_{M(x_j)}^T \dot{\tilde{W}}_{M(x_j)} \\ &+ \sum_{i=1}^3 \beta_{C(x_j, \dot{x}_j)}^{-1} \tilde{W}_{C(x_j, \dot{x}_j)}^T \dot{\tilde{W}}_{C(x_j, \dot{x}_j)} \\ &+ \sum_{i=1}^3 \beta_{G(x_j)}^{-1} \tilde{W}_{G(x_j)}^T \dot{\tilde{W}}_{G(x_j)} \end{aligned} \quad (34)$$

By substituting equation (31) into equation (34), we obtain:

$$\begin{aligned} \dot{V}(t) &= \frac{1}{2} \sum_{i=1}^3 s_i \dot{M}(x_j) \alpha_i s_i + s_1 \alpha_1 K_I \int_0^t s_1 dt \\ &+ \sum_{i=1}^3 s_i \left[ \tilde{f}_i(X) - \tau_{s1} - \tau_l - \tau_p + E_i(X) + \sigma_{di} \right. \\ &\quad \left. - C(x_j, \dot{x}_j) \alpha_i s_i \right] \end{aligned}$$

$$\begin{aligned} &+ \sum_{i=1}^3 \beta_{M(x_j)}^{-1} \tilde{W}_{M(x_j)}^T \dot{\tilde{W}}_{M(x_j)} \\ &+ \sum_{i=1}^3 \beta_{C(x_j, \dot{x}_j)}^{-1} \tilde{W}_{C(x_j, \dot{x}_j)}^T \dot{\tilde{W}}_{C(x_j, \dot{x}_j)} \\ &+ \sum_{i=1}^3 \beta_{G(x_j)}^{-1} \tilde{W}_{G(x_j)}^T \dot{\tilde{W}}_{G(x_j)} \end{aligned} \quad (35)$$

Apply property 2 and replace  $\dot{\tilde{W}}_{M(x_j)} = -\dot{\hat{W}}_{M(x_j)}$ ,  $\dot{\tilde{W}}_{C(x_j, \dot{x}_j)} = -\dot{\hat{W}}_{C(x_j, \dot{x}_j)}$ ,  $\dot{\tilde{W}}_{G(x_j)} = -\dot{\hat{W}}_{G(x_j)}$  into (35) we have:

$$\begin{aligned} \dot{V}(t) &= \sum_{i=1}^3 s_i [-\tilde{M}_R(x_j)\alpha_i\ddot{x}_{rj} - \tilde{M}_R(x_j)\alpha_i\lambda_i\dot{x}_{rj} \\ &- \tilde{C}_R(x_j, \dot{x}_j)\alpha_i\dot{x}_{rj} - \tilde{C}_R(x_j, \dot{x}_j)\alpha_i\lambda_i x_{rj} + \tilde{M}_R(x_j)\alpha_i\lambda_i \\ &+ \tilde{C}_R(x_j, \dot{x}_j)\alpha_i\lambda_i x_j - \tilde{G}_R(x_j)\alpha_i - \tau_{s1} - \tau_p + E_i(X) + \sigma_{di}] \\ &- \sum_{i=1}^3 \beta_{M(x_j)}^{-1} \tilde{W}_{M(x_j)}^T \dot{\hat{W}}_{M(x_j)} \\ &- \sum_{i=1}^3 \beta_{C(x_j, \dot{x}_j)}^{-1} \tilde{W}_{C(x_j, \dot{x}_j)}^T \dot{\hat{W}}_{C(x_j, \dot{x}_j)} \\ &- \sum_{i=1}^3 \beta_{G(x_j)}^{-1} \tilde{W}_{G(x_j)}^T \dot{\hat{W}}_{G(x_j)} \end{aligned} \quad (36)$$

By substituting equation (26) into equation (36), we obtain:

$$\begin{aligned} \dot{V}(t) &= \sum_{i=1}^3 \alpha_i s_i \tilde{W}_{M(x_j)}^T h_{M(x_j)} (-\ddot{x}_{rj} - \lambda_i\dot{x}_{rj} + \lambda_i\dot{x}_j) \\ &+ \sum_{i=1}^3 \alpha_i s_i \tilde{W}_{C(x_j, \dot{x}_j)}^T h_{C(x_j, \dot{x}_j)} (-\dot{x}_{rj} - \lambda_i x_{rj} + \lambda_i x_j) \\ &- \sum_{i=1}^3 \alpha_i s_i \tilde{W}_{G(x_j)}^T h_{G(x_j)} \\ &- \sum_{i=1}^3 s_i [\alpha_1 K_{s1} \text{sign}(s_1) - E_i(X) - \sigma_{di}] - \alpha_1 s_1 K_P s_1 \\ &- \sum_{i=1}^3 \beta_{M(x_j)}^{-1} \tilde{W}_{M(x_j)}^T \dot{\hat{W}}_{M(x_j)} \\ &- \sum_{i=1}^3 \beta_{C(x_j, \dot{x}_j)}^{-1} \tilde{W}_{C(x_j, \dot{x}_j)}^T \dot{\hat{W}}_{C(x_j, \dot{x}_j)} \\ &- \sum_{i=1}^3 \beta_{G(x_j)}^{-1} \tilde{W}_{G(x_j)}^T \dot{\hat{W}}_{G(x_j)} \end{aligned} \quad (37)$$

Chose  $K_{s1} \geq \frac{1}{\alpha_1} |E_1(X) + E_2(X) + E_3(X) + \sigma_{d1} + \sigma_{d2} + \sigma_{d3}|$  and replace adaptive law (30) into the equation (35) we obtain:

$$\begin{aligned} \dot{V}(t) &= -\alpha_1 s_1^2 K_P - \alpha_1 |s_1| K_{s1} + \sum_{i=1}^3 s_i [E_i(X) + \sigma_{di}] \\ &\leq -\alpha_1 s_1^2 K_P \leq 0 \end{aligned} \quad (38)$$

Select  $K_1 \geq \frac{1}{\alpha_1} [E_1(X) + E_2(X) + E_3(X) + \sigma_{d1} + \sigma_{d2} + \sigma_{d3}]$  furthermore, by substituting equations (28) and (30) into equation (35), we obtain:

$$\begin{aligned} \dot{V}(t) &= -\alpha_1 s_1^2 K_P - \alpha_1 s_1 K_1 + \sum_{i=1}^3 s_i [E_i(X) + \sigma_{di}] \\ &\leq -\alpha_1 s_1^2 K_P \leq 0 \end{aligned} \quad (39)$$

Where: all parameters of the adaptive control system are bounded with  $\tau > 0$ , and all initial conditions are bounded at  $t = 0, 0 \leq V(0) \leq \infty$  is ensured. We have:

$$\int_0^\infty \alpha_1 s_1^2 K_P dt \leq - \int_0^\infty \dot{V}(t) dt \leq V(0) - V(\infty) \quad (40)$$

We have:

$$\lim_{t \rightarrow \infty} \int_0^t \alpha_1 s_1^2 K_P dt < \infty \tag{41}$$

According to Barbalat’s Lemma, it can be shown that  $\lim_{t \rightarrow \infty} \int_0^t \alpha_1 s_1^2 K_P dt = 0$ . The fact that  $s_1 \in L^\infty, \dot{s}_1 \in L^\infty$ , thus  $s_1 \rightarrow 0$  when  $t \rightarrow \infty$ , hence  $\dot{e}_1 \rightarrow 0$  when  $t \rightarrow \infty$ . The proof is completed.

Where: With the desired value  $x_{r1}, x_{r3}, x_{r5}$  converged to 0 when  $t \rightarrow \infty$ , the system is stable by the adapting control law (32).

#### 4. SIMULATION RESULTS

The controller has been designed to be simulated in software MATLAB/Simulink. The system parameters are used in Table 1. Simulation forklift desired location  $x_{r1} = 1m$  and  $x_{r3} = 0rad, x_{r5} = 0rad, \sigma_d = 0N$ .

Table 1. Symbols and parameters value of the ECGS

Symbol	Describe	Value	Unit
$M$	Weight of trolley	24	Kg
$m_1$	Weight of hook	7	Kg
$m_2$	Weight of electrolytic plate	10	Kg
$l_1$	Length of cable hook	2	m
$l_2$	Length of electrolytic plate	0.6	m
$g$	Gravitational constant	9.81	m/s <sup>2</sup>
$\mu$	Coefficient of friction	0.2	N/m/s

Apply genetic algorithms (GA) to find the optimal values of sliding mode controller satisfying the objective function (40):

$$J = \int e_1^2(t)dt + \int e_2^2(t)dt + \int e_3^2(t)dt \rightarrow \min \tag{42}$$

Parameters of GA in this study were selected as follows: Evolution over 10 generations; Population size 5000; Coefficient of hybridization 0.6; Mutation coefficient 0.4. We received the following parameters:

$$\lambda_1 = 1, \lambda_2 = 0.03, \lambda_3 = 2.14, \alpha_1 = 1, \alpha_2 = 1.63, \alpha_3 = 0.26, k_s = 0.43.$$

From (10 - 12) we choose:  $\delta_1 = \delta_2 = \delta_3 = 0.5$ .

From (31) we choose:

$$K_P = 12, K_I = 0.001, K_{S1} = 0.32.$$

Amplification coefficient in the adaptive law (30) is selected as follows:

$$\beta_{M(x_1)} = 80, \beta_{M(x_3)} = 1000, \beta_{M(x_5)} = 1920,$$

$$\beta_{G(x_1)} = \beta_{G(x_3)} = \beta_{G(x_5)} = 1$$

$$\beta_{C(x_1, x_1)} = 1360, \beta_{C(x_3, x_3)} = \beta_{C(x_5, x_5)} = 0.01$$

The simulation results of all the controllers are shown in Figures (6-8).

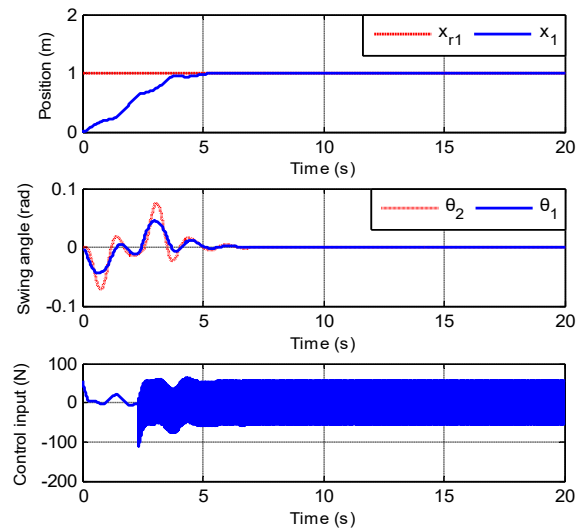


Figure 6. The simulation results of the ECGS when using Neural sliding mode controller

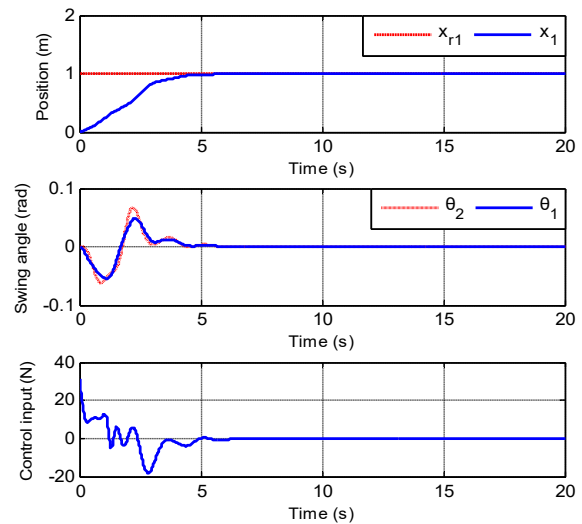


Figure 7. The simulation results of the ECGS when using Fuzzy sliding mode controller

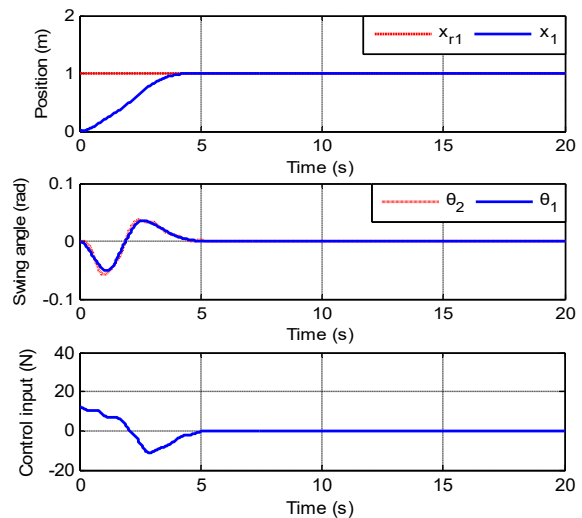


Figure 8. The simulation results of the ECGS when using adaptive SMC sustainable on the basis of fuzzy neurons

Based on the results of the simulation Figure 8, it can be seen that Maximum% overshoot for  $x_1$  (POT) 0%, Settling time for  $x_1$  ( $t_{x1}$ ) 4.15s; Maximum control input ( $F_{max}$ ) 12N, Settling time for  $F$  ( $t_F$ ) 5s; Maximum swing angle of hook ( $\theta_{1max}$ ) 0.05 (rad), Settling time for ( $t_{\theta1}$ ) 4.68s; Maximum swing angle of electrolytic plate ( $\theta_{2max}$ ) 0.05 (rad), Settling time for ( $t_{\theta2}$ ) 5s.

In order to clarify the superiority of the solution, the authors compared the adaptive sliding mode controller on the basis of the fuzzy neurons shown in Figure 8 with other well designed control methods simulated in Figures 6, 7 as shown in Table 2.

Table 2. Comparison of adaptive sliding mode controllers on the basis of fuzzy neurons with other control methods designed

Symbol	Figure 6	Figure 7	Figure 8
POT	0%	0%	0%
$F_{max}$	112N	32N	12N
$t_F$	$\infty$	6.3s	5s
$t_{x1}$	5.3s	5.6s	4.15s
$t_{\theta1}$	6.3s	5.7s	4.68s
$t_{\theta2}$	6.7s	5.7s	5s
$\theta_{1max}$	0.046 rad	0.055 rad	0.05 rad
$\theta_{2max}$	0.075 rad	0.069 rad	0.055 rad

Based on the results in Table 2, it can be seen that the study group utilized an adaptive sliding mode controller on the basis of fuzzy neurons is optimal.

In fact when the system gantry cranes working electrolytic copper, there are interference impacts to the system. In order to test the reliability of the adaptive sliding mode controller sustainable on the basis of fuzzy neurons, the author assumes the steps of the interfering signal to the crane system at specific times as follows: First (time step = 10s,  $\sigma_d = 5N$ , time = 2s); Second (step time = 10s,  $\theta_d = x_{r5} = 0.1rad$ , time = 2s). Simulation results are shown in Figure 9.

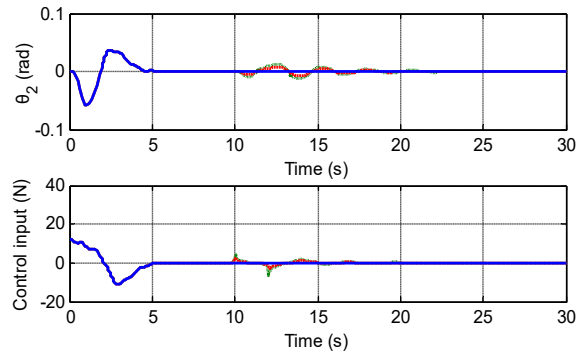
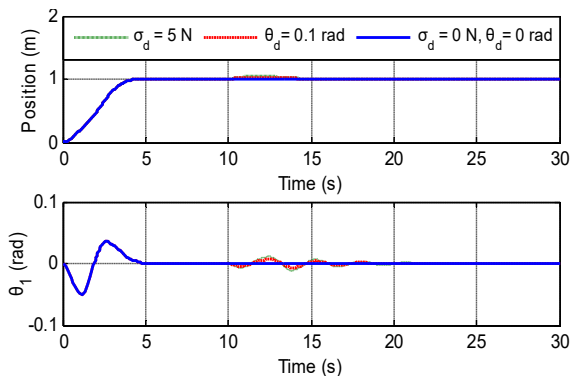


Figure 9. The simulation results of the ECGCS when the system has interference

When the ECGCS is working, the parameters of length and weight of the load are constantly changing. To keep abreast with the real situation and study the impact of adaptive sliding mode controller sustainable on the basis of fuzzy neurons, the system parameters are changed as follows: First change  $l_2 = 0.4m, m_2 = 8Kg$ , the other system parameters in Table 1 do not change. Second change  $l_2 = 0.8m, m_2 = 12Kg$ , the other system parameters in Table 1 do not change. Simulation results are shown in Figure 10.

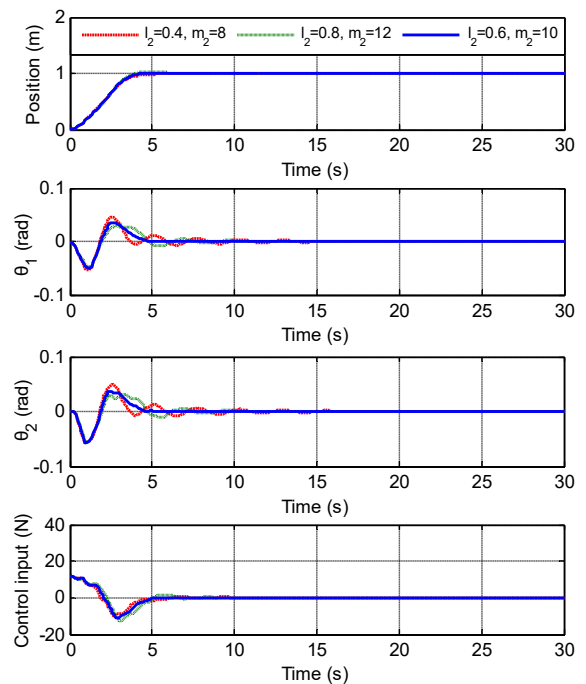


Figure 10. The simulation results of the ECGCS when the system parameters change

Based on the simulated results that shown in Figures 9 and 10, we can see that, when the disturbances affecting the system and the parameters change, the proposed control system can control the vibration of the small load and achieve the desired position in a short time.

## 5. CONCLUSION

In this paper, a sliding mode controller have designed to control the copper electrolytic gantry crane system to move to the desired position quickly and control the vibration of the electrolyte plate. However, there is the chattering phenomenon around the slip surface. To overcome this drawback fuzzy sliding controller have designed in order to increase the cling efficiency, increase the convergence speed, the adaptive sliding mode controller sustainable on the basis of neurons (RBFNNs) is designed to estimate online the nonlinear function in control law and use fuzzy logic to estimate the amplitude of the control law. Based on the stability theory Lyapunov, we have proven that the proposed control system is always stable throughout the work area. The efficiency of the controller has been tested through simulation of MATLAB / Simulink. Simulation results show that the quality of the adaptive sliding mode controller sustainable on the basis of fuzzy neurons is better than that of other controllers. To test the reliability of the control method, we simulated when the system parameters change and there are interference disturbances on the system. The results also show that the copper electrolytic crane can move to the desired position quickly and control the oscillation of the small load. From the simulation results we can continue to study to put into practice.

## REFERENCES

- [1]. J. Smoczek, "Interval arithmetic-based fuzzy discrete-time crane control scheme design," *Bull. Pol. Ac. Tech.*, 61 (4), 863-870, 2013.
- [2]. Van Trung Nguyen, Chunhua Yang, Chenglong Du, Liqing Liao, "Design and Implement of Finite-Time Sliding Mode Controller for Fuzzy Overhead Crane System," *ISA Transactions*, 124, 374-385, 2022.
- [3]. Ernesto Molina-Santana, Michel Roberto Ferrer-Cepero, Felipe Gonzalez-Montañez, Jesús Ulises Liceaga-Castro, Victor M. Jimenez-Mondragon, Juan Carlos Olivares-Galvan, "Generalized framework for designing a linear control scheme for regulating a sub-actuated overhead crane," *International Journal of Dynamics and Control*, 13:168, 2025.
- [4]. S. Zhang, X. He, H. Zhu, Q. Chen, Y. Feng, "Partially saturated coupled-dissipation control for underactuated overhead cranes," *Mechanical Systems and Signal Processing*, 136: 106449, 2020. DOI 10.1016/j.ymsp.2019.106449.
- [5]. G. Rigatos, "Nonlinear optimal control for the underactuated double-pendulum overhead crane," *Journal of Vibration Engineering & Technologies*, 1-21, 2023. DOI 10.1007/s42417-023-00902-y.
- [6]. M. R. Mojallizadeh, B. Brogliato, C. Prieur, "Modeling and control of overhead cranes: A tutorial overview and perspectives," *Annual Reviews in Control*, 56: 100877, 2023. DOI 10.1016/j.arcontrol.2023.03.002.
- [7]. N. Sun, Y.C. Fang, X.B. Zhang, "Energy coupling output feedback control of 4-DOF underactuated cranes with saturated inputs," *Automatica*, 49 (5), 1318-1325, 2013.
- [8]. Y.C. Fang, B.J. Ma, P.C. Wang, X.B. Zhang, "A motion planning-based adaptive control method for an underactuated crane system," *IEEE Trans. on Control Systems Technology*, 20 (1), 241-248, 2012.
- [9]. Khalid L. Sorensen, William Singhose, Stephen Dickerson, "A controller enabling precise positioning and sway reduction in bridge and gantry cranes," *Control Engineering Practice*, 15, 825-837, 2007.
- [10]. M.A. Ahmad, A.N.K. Nasir, N. Hambali, H. Ishak, "Hybrid Input Shaping and PD-type Fuzzy Logic Control Scheme of a Gantry Crane System," in *18th IEEE International Conference on Control Applications Part of 2009 IEEE Multi-conference on Systems and Control*, Saint Petersburg, Russia, 2009.
- [11]. Menghua Zhang, Xin Ma, Xuewen Rong, Xincheng Tian, Yibin Li, "Adaptive tracking control for double-pendulum overhead cranes subject to tracking error limitation, parametric uncertainties and external disturbances," *Mechanical Systems and Signal Processing*, 76-77, 15-32, 2016.
- [12]. Mohammad Javad Maghsoudi, Z. Mohamed, A.R. Husain, M.O. Tokhi, "An optimal performance control scheme for a 3D crane," *Mechanical Systems and Signal Processing*, 66-67, 756-768, 2016.
- [13]. Zhe Sun, Ning Wang, Yunrui Bi, Jinhui Zhao, "A DE based PID controller for two dimensional overhead crane," in *Proceedings of the 34th Chinese Control Conference*, Hangzhou, China, 2015.
- [14]. Mahmud Iwan Solihin, Wahyudi, Ari Legowo, Rini Akmeliawati, "Robust PID Anti-swing Control of Automatic Gantry Crane based on Kharitonov's Stability," in *2009 4th IEEE Conference on Industrial Electronics and Applications*, 2009.
- [15]. Mahmud Iwan Solihin, Wahyudi, M.A.S. Kamal, Ari Legowo, "Objective Function Selection of GA-Based PID Control Optimization for Automatic Gantry Crane," in *2008 International Conference on Computer and Communication Engineering*, Kuala Lumpur, Malaysia, 2008.
- [16]. Mahmud Iwan Solihin, Wahyudi, "Fuzzy-tuned PID Control Design for Automatic Gantry Crane," in *2007 International Conference on Intelligent and Advanced Systems*, Kuala Lumpur, Malaysia, 2007.
- [17]. E. A. Esleman, G. Önal, M. Kalyoncu, "Optimal PID and fuzzy logic based position controller design of an overhead crane using the Bees Algorithm," *SN Applied Sciences*, 3(10): 811, 2021. DOI: <https://doi.org/10.1007/s42452-021-04793-0>.
- [18]. Jaroslaw Smoczek, "Experimental verification of a GPC-LPV method with RLS and P1-TS fuzzy-based estimation for limiting the transient and residual vibration of a crane system," *Mechanical Systems and Signal Processing*, 62-63, 324-340, 2015.
- [19]. Dianwei Qian, Shiwen Tong, Suk Gyu Lee, "Fuzzy-Logic-based control of payloads subjected to double-pendulum motion in overhead cranes," *Automation in Construction*, 65, 133-143, 2016.

- [20]. Cheng-Yuan Chang, "Adaptive Fuzzy Controller of the Overhead Cranes With Nonlinear Disturbance," *IEEE Transactions on Industrial Informatics*, 3, 2, 2007.
- [21]. Naif B. Almutairi, Mohamed Zribi, "Fuzzy Controllers for a Gantry Crane System with Experimental Verifications," *Mathematical Problems in Engineering*, 2016. DOI: 10.1155/1965923.
- [22]. Lifu Wang, Hongbo Zhang, Zhi Kong, "Anti-swing Control of Overhead Crane Based on Double Fuzzy Controllers," in *2015 27<sup>th</sup> Chinese Control and Decision Conference (CCDC)*, 2015.
- [23]. Xiao-jing Wang, Zhi-mei Chen, "Two-degree-of-freedom Sliding Mode Anti-swing and Positioning Controller for Overhead Cranes," in *28<sup>th</sup> Chinese Control and Decision Conference (CCDC)*, 2016.
- [24]. Le Anh Tuan, Soon-Geul Lee, "Sliding mode controls of double-pendulum crane systems," *Journal of Mechanical Science and Technology*, 27 (6), 1863~1873, 2013. DOI 10.1007/s12206-013-0437-8.
- [25]. Cheng-Yuan Chang, Kou-Cheng Hsu, Kuo-Hung Chiang, Guo-En Huang, "An Enhanced Adaptive Sliding Mode Fuzzy Control for Positioning and Anti-Swing Control of the Overhead Crane System," in *IEEE International Conference on Systems, Man, and Cybernetics*, Taipei, Taiwan, 2006.
- [26]. Lingzhi Cao, Lei Liu, "Adaptive Fuzzy Sliding Mode Method-Based Position and Anti-swing Control for Overhead Cranes," in *2011 Third International Conference on Measuring Technology and Mechatronics Automation*, 2011. DOI 10.1109/ICMTMA.2011.85.
- [27]. Lun-Hui Lee, Pei-Hsiang Huang, Yu-Cheng Shih, Sung-Chih Ku, Cheng-Yuan Chang, "Adaptive Fuzzy Sliding Mode Control to Overhead Crane by CCD Sensor," in *2011 IEEE International Conference on Control Applications (CCA) Part of 2011 IEEE Multi-Conference on Systems and Control Denver*, 2011.
- [28]. Quang Hieu Ngo, Ngo Phong Nguyen, Chi Ngon Nguyen, Thanh Hung Tran, Keum-Shik Hong, "Fuzzy Sliding Mode Control of Container Cranes," *International Journal of Control, Automation, and Systems*, 13(2):419-425, 2015. DOI 10.1007/s12555-014-0150-0.
- [29]. S. Pezeshki, M. A. Badamchizadeh, A. R. Ghiasi, S. Ghaemi, "Control of Overhead Crane System Using Adaptive Model-Free and Adaptive Fuzzy Sliding Mode Controllers," *J Control Autom Electr Syst*, 26:1-15, 2015. DOI 10.1007/s40313-014-0152-4.
- [30]. Diantong Liu, Jianqiang Yi, Dongbin Zhao, Wei Wang, "Adaptive sliding mode fuzzy control for atwo-dimensional overhead crane," *Mechatronics*, 15, 505-522, 2025.
- [31]. Manh-Linh Nguyen, Hoang-Phat Nguyen, Thi-Van-Anh Nguyen, "H-Infinity Approach Control on Takagi-Sugeno Fuzzy Model for 2-D Overhead Crane System," *Journal of Applied Science and Engineering*, 28, 5, 995-1003, 2024.
- [32]. Q. Zhang, B. Fan, L. Wang, Z. Liao, "Fuzzy sliding mode control on positioning and anti-swing for overhead crane," *International Journal of Precision Engineering and Manufacturing*, 24(8): 1381-1390, 2023. DOI 10.1007/s12541-023-00828-1.
- [33]. V. T. Nguyen, C. Yang, C. Du, L. Liao, "Design and implementation of finite time sliding mode controller for fuzzy overhead crane system," *ISA Transactions*, 124: 374-385, 2022. DOI 10.1016/j.isatra.2019.11.037.
- [34]. Dian-Tong Liu, Wei-Ping Guo, Jian-Qiang Yi, Dong-Bin Zhao, "Double-Pendulum-Type overhead crane dynamics and ITS adaptive sliding mode fuzzy control," in *Proceedings of the Third International Conference on Machine Learning and Cybernetics*, Shanghai, 2004.
- [35]. Oguz Yakut, "Application of intelligent sliding mode control with moving sliding surface for overhead cranes," *Neural Comput & Applic*, 24:1369-1379, 2014. DOI 10.1007/s00521-013-1351-9.
- [36]. Zhiqiang Ma, Guanghui Sun, "Dual terminal sliding mode control design for rigid robotic manipulator," *Journal of the Franklin Institute*, 000, 1-23, 2017.